Chemical Shielding Tensor of a Carbene†

Anthony J. Arduengo, III,*,‡ David A. Dixon,*,‡ Kristin K. Kumashiro,§ Chengteh Lee,∥ William P. Power,§,⊥ and Kurt W. Zilm*,§

Contribution from the DuPont Science and Engineering Laboratory, Experimental Station, P. O. Box 80328, Wilmington, Delaware 19880-0328, Department of Chemistry, Yale University, 225 Prospect Street, P. O. Box 6666, New Haven, Connecticut 06511-8118, and Cray Research, Inc., 655 East Lone Oak Drive, Eagan, Minnesota 55121

Received December 27, 1993•

Abstract: The first experimental determination of the chemical shielding tensor of a singlet carbene center, 1,3,4,5-tetramethylimidazol-2-ylidene (**1**), is reported. Detailed *ab initio* theoretical calculations of the chemical shielding tensors are reported for local density functional theory (LDFT) and the Hartree–Fock levels (HF) in the LORG and IGLO frameworks. The chemical shielding anisotropy is quite large, which is characteristic of the lowest-energy-singlet carbene centers. The anisotropy at the carbene center in **1** is ~240 ppm. This is one of the largest anisotropies observed for carbon in a strictly organic framework. The calculations indicate that the orientation of the chemical shielding tensor of the carbene is such that the most shielded component is perpendicular to the molecular plane, with the intermediate component oriented approximately along the direction of the lone pair, and the least shielded component perpendicular to the other two. This orientation, as well as the relative size of the anisotropy, agrees with calculations on the singlet carbenes **1**, imidazol-2-ylidene (**2**), and $:CF_2$. The size of the anisotropy is predicted to be enhanced for the parent carbene $:CH_2$.

Introduction

Significant efforts have been expended to characterize and understand the electronic nature of carbenes.[1] These highly reactive species possess a unique chemistry among carbon compounds;[2-5] however, this reactivity has precluded much detailed study of their structure by conventional experimental means, generally permitting only simple interpretation of reaction products or kinetics. Absorption spectra have provided details of the structure of many simple carbenes, and theoreticians have been particularly active in providing descriptions of the electronic and molecular structure based on *ab initio* molecular orbital calculations.[6,7] While ESR spectroscopy has been successful in providing information about the electronic structure of several matrix-isolated triplet carbenes,[8] the electronic structure of ESR-silent singlet carbenes has yet to be fully investigated by spectroscopic means. We have recently reported the experimental and theoretical determination of the electron density in the stable singlet carbene 1,3,4,5-tetramethylimidazol-2-ylidene-d_{12}.[9]

One of the most successful techniques for providing structural and electronic information about closed-shell species is solid-state NMR spectroscopy. Coupled with matrix-isolation techniques, solid-state NMR has been used to identify various reactive intermediates in organic chemistry, through interpretation of isotropic chemical shifts[10,11] and identification of the number of protons bonded to the reactive species.[12] Characterization of the anisotropy or three-dimensional character of the chemical shielding provides an even more powerful probe of the electronic environment around the nucleus of interest, allowing the orientation of particular shielding or deshielding influences to be correlated with the local molecular structure. Such an approach is especially informative when coupled with theoretical predictions of the chemical shielding tensor.

Our preparation of a series of stable crystalline carbenes[13,14] has permitted us to investigate these normally transient species using solid-state NMR techniques in order to further characterize their electronic and structural features. In this report, we concentrate on experimental results for 1,3,4,5-tetramethylimidazol-2-ylidene (**1**). These results are then compared to *ab initio* molecular orbital and density functional calculations on **1** and the parent imidazol-2-ylidene (**2**) as well as the prototypical carbenes $:CH_2$ (**3**) and $:CF_2$ (**4**). Comparisons are also made with carbenium ions $\mathbf{1}\cdot H^+$ and $\mathbf{2}\cdot H^+$ that are derived from protonation of **1** and **2** respectively.

Experimental Section

Samples of **1**, prepared as described previously,[9,14] were sealed in 5-mm-o.d. glass tubes under helium. The precursor salt, 1,3,4,5-tetramethylimidazolium chloride[9,14] ($\mathbf{1}\cdot H^+ Cl^-$), was packed under argon into a zirconia rotor. Carbon-13 solid-state NMR spectra were obtained with cross-polarization (CP), high-power proton decoupling, and magic-angle spinning (MAS) on both a custom-built 7.05-T NMR spectrometer operating at 75 MHz for ^{13}C and a custom-built 2.35 T NMR spectrometer operating at 25 MHz for ^{13}C. Proton $\pi/2$ pulse widths were 5 μs, corresponding to a proton decoupling field of 50 kHz. A CP time of 3 ms was used for all samples at both fields. Acquisition times of 51 ms

† DuPont Contribution No. 6793.
‡ DuPont.
§ Yale University.
∥ Cray Research.
⊥ Current address: Department of Chemistry, University of Waterloo, Ontario, Canada N2L 3G1.
• Abstract published in *Advance ACS Abstracts*, June 1, 1994.

(1) Regitz, M. *Angew. Chem. Int. Ed. Engl.* **1991**, *30*, 674.
(2) Baron, W. J.; Bertoniere, N. R.; DeCamp, M. R.; Griffin, G. W.; Hendrick, M. E.; Jones, M., Jr.; Levin, R. H.; Moss, R. A.; Sohn, M. B. Carbenes. In *Carbenes*; Jones, M., Jr., Moss, R. A., Eds.; John Wiley & Sons: New York, 1973.
(3) Closs, G. L.; Gaspar, P. P.; Hammond, G. S.; Hartzler, H. D.; Mackay, C.; Seyferth, D.; Trozzolo, A. M.; Wasserman, E. Carbenes. In *Carbenes*; Moss, R. A., Jones, M., Jr., Eds.; John Wiley & Sons: New York, 1975.
(4) Kirmse, W. *Carbene Chemistry*; Academic Press, Inc.: New York, 1971; Vol. 1.
(5) Hine, J. *Divalent Carbon*; The Ronald Press Co.: New York, 1964.
(6) Harrison, J. F. *Acc. Chem. Res.* **1974**, *7*, 378.
(7) Schaefer, H. F., III. *Science* **1986**, *231*, 1100 and references therein.
(8) Perutz, R. N. *Chem. Rev.* **1985**, *85*, 77.
(9) Arduengo, A. J., III; Dias, H. V. R.; Dixon, D. A.; Harlow, R. L.; Klooster, W. T.; Koetzle, T. F. *J. Am. Chem. Soc.*, in press.
(10) Zilm, K. W.; Merrill, R. A.; Greenberg, M. M.; Berson, J. A. *J. Am. Chem. Soc.* **1987**, *109*, 1567.
(11) Greenberg, M. M.; Blackstock, S. C.; Berson, J. A.; Merrill, R. A.; Duchamp, J. C.; Zilm, K. W. *J. Am. Chem. Soc.* **1991**, *113*, 2318.
(12) Zilm, K. W.; Merrill, R. A.; Webb, G. G.; Greenberg, M. M.; Berson, J. A. *J. Am. Chem. Soc.* **1989**, *111*, 1533.
(13) Arduengo, A. J.; Harlow, R. L.; Kline, M. *J. Am. Chem. Soc.* **1991**, *113*, 361.
(14) Arduengo, A. J., III; Dias, H. V. R.; Harlow, R. L.; Kline, M. *J. Am. Chem. Soc.* **1992**, *114*, 5530.

0002-7863/94/1516-6361$04.50/0

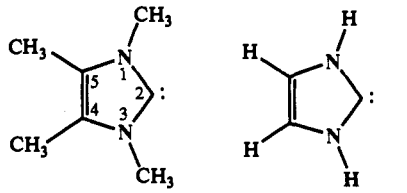

1

2

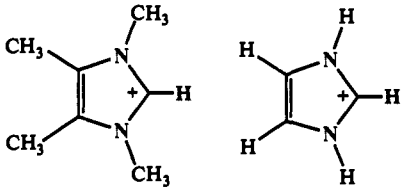

1·H+

2·H+

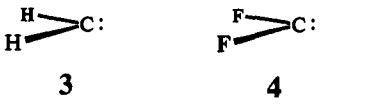

3 4

were used, during which 2048 complex data points were collected. Magic-angle spinning rates up to 2.5 kHz in custom-built double-resonance MAS probes at each field strength were used to assign the isotropic peaks of **1**. A Doty Scientific double-resonance MAS probe for the 7.05-T spectrometer was used to spin samples of the precursor at rates up to 5 kHz. Carbon-13 CP/MAS spectra of **1** at 25 MHz were collected at both room temperature (293 K) and 90 K; spectra at 75 MHz were collected at room temperature only. All spectra are referenced with respect to tetramethylsilane (TMS); this was accomplished using external samples of adamantane and hexamethylbenzene.

Theoretical Calculations

The density functional theory calculations[15-19] were done with the program DGauss,[20-22] which employs Gaussian basis sets on a Cray YMP computer. The basis sets for C, N, and F are triple-ζ in the valence space augmented with a set of polarization functions with the form (7111/411/1).[23] The auxiliary fitting basis set for the electron density and the exchange-correlation potential has the form [8/4/4]. For H, a polarized triple-ζ valence basis set was used with the form (311/1) together with an auxiliary fitting basis set of the form [4/1]. This basis set is labeled TZVP. The calculations were done at the local density functional level with the local potential of Vosko, Wilk, and Nusair.[24] For **2**, **3**, **4**, **1**·H+ and **2**·H+, the geometries were optimized with this basis set at the self-consistent gradient-corrected (nonlocal) level with the nonlocal exchange potential of Becke[25-27] together with the nonlocal correlation functional of Perdew[28] (BP). Following our work on analysis of the electron density of the carbene **1**, we used its experimental geometry from a neutron diffraction study.[9]

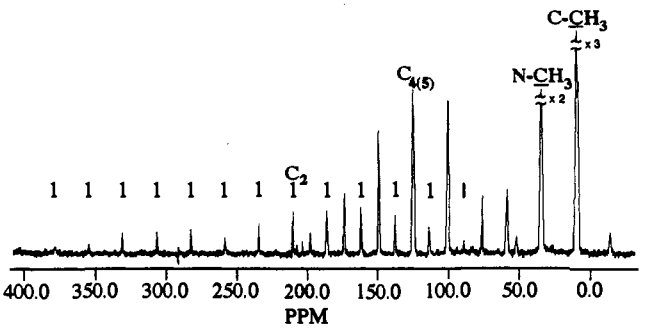

Figure 1. Carbon-13 CP/MAS spectrum of **1**, with spinning of 1.8 kHz at 7.05 T and 293 K. The isotropic shifts of each carbon have been indicated on the spectrum. The spinning sidebands corresponding to the carbene site have been marked by a vertical line above the spectrum.

Calculations of the NMR shifts were done at the LDFT level in two ways. The calculations handle the gauge invariance problem in terms of the localized orbital/local origin (LORG)[29] and individual gauge localized orbital (IGLO)[30-32] methods following the recent derivation of Lee[33] based on the work of Salahub and co-workers[34] and Handy and co-workers.[35] Calculations were done with the TZVP basis set described above.

The calculations at the Hartree–Fock level were done with the program CADPAC.[36] Two basis sets were used. The first is of polarized double-ζ quality (DZP).[37] For all molecules except for **1** and **1**·H+, calculations were also done with a triple-ζ basis set augmented by two sets of polarization functions (TZ2P).[38] For **1** and **1**·H+, a TZ2P calculation cannot be done in CADPAC (369 basis functions). Because our focus is on the ring atoms and primarily on C_2, calculations on **1** and **1**·H+ were done with a modified TZ2P basis set denoted as "*TZ2P*". The "*TZ2P*" basis set had a TZ2P basis set for the ring atoms, a DZP basis set for the methyl carbons, and DZ for H except for the unique hydrogen at C_2 of **1**·H+, for which a DZP basis set was used.[39,40] Chemical shielding calculations were done at the coupled perturbed Hartree–Fock level (CPHF) and at the IGLO and LORG levels.

Results and Discussion

A ^{13}C CP/MAS spectrum of the carbene **1** is shown in Figure 1. The isotropic shift of the carbene carbon in the solid, 209.6 ppm, is very similar to that observed in solution for this compound, 213.7 ppm.[14] The other isotropic peaks in the solid-state spectrum closely match the solution data, appearing at 124.7 ppm ($C_{4(5)}$), 34.6 ppm (N-CH_3), and 9.5 ppm (C-CH_3). The solid-state and solution isotropic shifts for the carbons in **1** and **1**·H+ are given in Table 1 along with the predicted values from various theoretical

(15) Parr, R. G.; Yang, W. *Density Functional Theory of Atoms and Molecules*; Oxford University Press: New York, 1989.
(16) Salahub, D. R. In *Ab Initio Methods in Quantum Methods in Quantum Chemistry-II*; Lawlwy, K. P., Ed.; J. Wiley & Sons: New York, 1987; p 447.
(17) Wimmer, E.; Freeman, A. J.; Fu, C.-L.; Cao, P.-L.; Chou, S.-H.; Delley, B. *Supercomputer Research in Chemistry and Chemical Engineering*; ACS Symposium Series 353, American Chemical Society: Washington, DC, 1987.
(18) Jones, R. O.; Gunnarsson, O. *Rev. Mod. Phys.* **1989**, *61*, 689.
(19) Zeigler, T. *Chem. Rev.* **1991**, *91*, 651.
(20) Andzelm, J. W.; Wimmer, E.; Salahub, D. R. *The Challenge of d and f Electrons: Theory and Computation*; ACS Symposium Series 394, American Chemical Society: Washington, DC, 1989.
(21) Andzelm, J. W. *Density Functional Methods in Chemistry*; Springer-Verlag: New York, 1991.
(22) Andzelm, J. W.; Wimmer, E. *J. Chem. Phys.* **1992**, *96*, 1280.
(23) Godbout, N.; Salahub, D. R.; Andzelm, J. W.; Wimmer, E. *Can. J. Chem.* **1992**, *70*, 560.
(24) Vosko, S. J.; Wilk, L.; Nusair, M. *Can. J. Phys.* **1980**, *58*, 1200.
(25) Becke, A. D. *Phys. Rev. A* **1988**, *38*, 3098.
(26) Becke, A. D. *The Challenge of d and f Electrons: Theory and Computation*; ACS Symposium Series 394, American Chemical Society: Washington, DC, 1989.
(27) Becke, A. D. *Int. J. Quantum Chem., Quantum. Chem. Symp.* **1989**, *23*, 599.
(28) Perdew, J. P. *Phys. Rev. B* **1986**, *33*, 8822.
(29) Hansen, A. E.; Bouman, T. D. *J. Chem. Phys.* **1985**, *82*, 5035.
(30) Kutzelnigg, W. *Isr. J. Chem.* **1980**, *19*, 193.
(31) Schindler, M.; Kutzelnigg, W. *J. Chem. Phys.* **1982**, *76*, 1919.
(32) Kutzelnigg, W.; Fleischer, U.; Schindler, M. The IGLO-Method: Ab-Initio Calculation and Interpretation of NMR Chemical Shifts and Magnetic Susceptibilities. In *NMR Basic Principles and Progress*; Diehl, P., Fluck, E., Gunther, H., Kosfeld, R., Seelig, J., Eds.; Springer: Berlin, 1991; p 165.
(33) Lee, C.; Fitzgerald, G.; Dixon, D. A.; Kleier, D. A. *J. Phys. Chem.*, submitted.
(34) Malkin, V. G.; Malkina, O. L.; Salahub, D. R. *Chem. Phys. Lett.* **1993**, *204*, 80,87.
(35) Smith, C. M.; Amos, R. D.; Handy, N. C. *Mol. Phys.* **1992**, *77*, 381.
(36) Amos, R. D.; Rice, J. E. *CADPAC*. The Cambridge Analytic Derivatives Package, Version 5.2, 1987.
(37) Dunning, T. H., Jr. *J. Chem. Phys.* **1970**, *53*, 2823. ζp(H) = 1.0; ζd(C) = 0.8; ζd(N) = 0.8; ζd(F) = 1.2.
(38) Dunning, T. H., Jr. *J. Chem. Phys.* **1971**, *55*, 716. ζp(H) = 1.5, 0.5; ζd(C) = 1.2, 0.4; ζd(N) = 1.35, 0.45; ζd(F) = 2.0, 0.6667.
(39) The use of "locally dense" basis set schemes has been previously described for NMR shielding calculations, see ref 40 and the following: Chesnut, D. B.; Moore, K. D. *J. Comput. Chem.* **1989**, *1989*, 648.
(40) Chesnut, D. B.; Rusiloski, B. E.; Moore, K. D.; Egolf, D. A. *J. Comput. Chem.* **1993**, *14*, 1364.

Table 1. Experimental and Calculated[a] Chemical Shifts[b] (ppm) in **1** and **1**·H$^+$

	experimental		HF/DZP		HF/"*TZ2P*"[d]		LDFT/TZVP	
	solution[c]	SS CP/MAS	IGLO	LORG	IGLO	LORG	IGLO	LORG
			1					
$^{13}C_2$	213.7	209.6	179.1	203.9	226.0	236.6	188.8	196.8
$^{13}C_{4(5)}$	123.1	124.7	105.9	124.4	112.6	122.5	101.1	106.2
$N^{13}CH_3$	35.2	34.6	16.5	28.0	26.0	30.7	28.6	33.6
$C^{13}CH_3$	9.0	9.5	-6.0	6.9	2.5	7.8	3.9	7.2
$^{15}N_{1(3)}$	-198.5		-230.9	-215.0	-216.5	-207.5	-193.9	-195.3
NC^1H_3	3.48		-11.3	1.1	-8.3	-1.5	-1.0	6.6
CC^1H_3	2.01		-12.9	0.4	-9.9	-2.5	-1.9	4.6
			1·H$^+$					
$^{13}C_2$	135.0	137.0	126.7	139.7	136.6	143.0	121.2	127.0
$^{13}C_{4(5)}$	126.8	129.7, 127.6	116.7	135.3	123.4	133.2	123.2	127.3
$N^{13}CH_3$	32.7	35.3, 34.0	20.4	32.3	29.7	34.4	33.5	38.6
$C^{13}CH_3$	7.3	9.9, 7.0	-4.4	8.4	4.2	9.2	7.7	10.6
$^{15}N_{1(3)}$	-206.6		-226.0	-208.8	-211.4	-201.4	-198.4	-195.2
NC^1H_3	3.72		-10.5	2.1	-7.4	-0.6	-0.8	7.1
CC^1H_3	2.20		-12.2	1.0	-9.1	-1.8	-2.7	3.9
C_2-^1H	9.28		-9.0	7.2	0.6	7.3	-0.1	7.2

[a] Calculated absolute isotropic shieldings have been converted to chemical shifts by the relationships $\delta_{^{13}C} = 186.4 - \sigma_{iso}$;[42,43] $\delta_{^{15}N} = -131.8 - \sigma_{iso}$;[44] $\delta_{^1H} = 30.6 - \sigma_{iso} + 0.2\{\Delta\delta(CH_4 - TMS)\}$.[45] [b] References are $(CH_3)_4Si$ for ^1H and ^{13}C and 5 N $NH_4{}^+NO_3{}^-$ for ^{15}N. [c] Solution data for **1** were recorded from a THF-d_8 solution, and solution data for **1**·H$^+$ were recorded from DMSO-d_6. [d] The "*TZ2P*" basis set used for **1** and **1**·H$^+$ is TZ2P for C_2, $C_{4(5)}$, and $N_{1(3)}$, DZP for the methyl carbons, and DZ for H.

treatments. Note that only single peaks occur for each of the chemically distinct carbon sites in **1**, confirming that the molecule has a high degree of symmetry in the *C*2/*c* crystal lattice, with the molecule sitting on a 2-fold axis, as previously determined.[14] Nonequivalence of the two halves of the molecule would be expected to lead to a doubling of the methyl and alkene peaks. Such doubling is evident in the ^{13}C CP/MAS spectrum of the precursor salt, 1,3,4,5-tetramethylimidazolium chloride (**1**·H$^+$ Cl$^-$). In the solid-state spectrum of **1**·H$^+$ Cl$^-$, all peaks other than the methine carbon, C_2, are doubled (Table 1). These doubled resonances reflect the asymmetric environment that **1**·H$^+$ occupies in a general position of a $P2_1/c$ crystal lattice,[41] but the resonances are close to their corresponding solution values.

The only chemical shift that has changed appreciably between **1**·H$^+$ and **1** is that of C_2, the carbene center; the other carbon (and nitrogen) nuclear environments appear to be relatively unaffected by the loss of the ring proton. The origin of this chemical shift change at C_2 is evident from the chemical shielding tensor at this center, as discussed below.

The spinning sidebands of the carbene peak in **1**, occurring at integer multiples of the spin rate to either side of the isotropic peak, cover a spectral width of approximately 300 ppm, indicating a large chemical shielding anisotropy for this site, with appreciable sideband intensity from near 90 ppm up to 360 ppm. By using Herzfeld–Berger analysis of the spinning sideband intensities,[46] it is possible to reconstruct the powder pattern and determine the three principal components of the carbon chemical shielding tensor. For this reconstruction, it is further necessary to assume that dipolar contributions from the neighboring ^{14}N nuclei are negligible. Support for this assumption is found in the absence of any asymmetric splitting of the carbene signals due to coupling with the quadrupolar nitrogen nuclei at 7.05 T.[47] The small magnitude of the C–N dipolar coupling constant, calculated to be 860 Hz using the X-ray crystallographically determined bond length of 136.3 pm,[14] limits the error introduced by this assumption to <12 ppm in the derived chemical shielding tensor components. Including this potential margin of error, the three principal components of the carbene chemical shielding tensor are determined to be 370 ± 20, 177 ± 18, and 82 ± 15 ppm with respect to TMS. Similarly, we have analyzed the spinning sideband distribution of the alkene carbons and have derived a chemical shielding tensor with principal components of 119 ± 19, 192 ± 22, and 63 ± 17 ppm. The slightly higher margins of error are due to the fewer number of spinning sidebands available for this site, as well as the potential influence of the adjacent quadrupolar ^{14}N nuclei. However, similar to the results for the carbene site, there is no evidence of asymmetric splitting of the MAS lines for the alkene carbons, so we believe that such influence is minimal at 7.05 T.

We have also performed ^{13}C CP/MAS NMR experiments on **1** at low field (2.35 T) at both room (293 K) and low (90 K) temperature. The acquisition of spectra at low field allows us to amplify the influence of the neighboring quadrupolar ^{14}N nuclei, as their effect on the ^{13}C NMR spectra is inversely proportional to the strength of the applied field. Lowering the temperature will attenuate any molecular motions that may be occurring at room temperature and indicate whether the spectra obtained at 293 K have been motionally averaged to a significant extent. The low-temperature spectra are identical to those obtained at room temperature; thus, we are confident that motion (other than zero point) is not causing any reduction of the observed chemical shielding anisotropy. The low-field ^{13}C CP/MAS NMR spectra show small yet discernible splittings of the carbene, alkene, and N-CH_3 peaks due to dipolar coupling between these carbon nuclei and the ^{14}N nuclei in the molecule.[48] As these splittings are present at both room and low temperature, they cannot be due to a change in the crystal structure or phase transition between 90 and 293 K. The magnitude of these ^{14}N-induced splittings of the ^{13}C resonances at $B_0 = 2.35$ T indicates that the influence of the ^{14}N quadrupolar interaction safely can be assumed to be negligible at $B_0 = 7.05$ T (that is, the high-field approximation is valid).

(41) Arduengo, A. J., III; Harlow, R. L.; Dias, H. V. R. unpublished results.
(42) Jameson, A. K.; Jameson, C. J. *Chem. Phys. Lett.* **1987**, *134*, 461.
(43) A more recent estimate of $\sigma^{13CO}(300\ K) = 0.6 \pm 0.9$ ppm *vs* the value of 1.0 ± 1.2 ppm used in ref 42 would lead to slightly different estimates for δ^{13C} from our calculated shieldings; see: Raynes, W. T.; McVay, R.; Wright, S. J. *J. Chem. Soc., Faraday Trans. 2* **1989**, *85*, 759.
(44) Jameson, C. T.; Jameson, A. K.; Oppusunggu, D.; Wille, S.; Burrell, P. M.; Mason, J. *J. Chem. Phys.* **1981**, *74*, 81.
(45) Raynes, W. T. Theoretical and Physical Aspects of Nuclear Shielding. In *Nuclear Magnetic Resonance*; Abraham, R. J., Ed.; The Chemical Society, Burlington House: London, 1978.
(46) Herzfeld, J.; Berger, A. E. *J. Chem. Phys.* **1980**, *73*, 6021.
(47) Hexem, J. G.; Frey, M. H.; Opella, S. J. *J. Chem. Phys.* **1982**, *77*, 3847.
(48) The values of the splittings and the intensities are as follows: C_2 (70 Hz, 1:1 doublet), $C_{4(5)}$ (145 Hz, 1:2 doublet, more intense peak at lower frequency), N-CH_3 (100 Hz, 1:2 doublet). The 1:1 doublet observed for C_2 is actually a 1:4:4 triplet for this AX_2 system, but the lowest intensity transition is not observed. This type of behavior for a ^{13}C center with two adjacent ^{14}N centers has been previously described; see: Olivieri, A. C.; Frydman, L.; Grasselli, M.; Diaz, L. E. *Magn. Reson. Chem.* **1988**, *26*, 281.

Table 2. Hartree–Fock-calculated NMR Shielding Tensors and Anisotropies at Carbene Centers in $^1A_1$ CH_2, CF_2, **1**, **1**·H^+, **2**, and **2**·H^+ [a,b]

molecule	basis	method	σ_{iso}	$\Delta\sigma$[c]	η[c]	σ_{11}	σ_{22}	σ_{33}
CH_2	DZP	CPHF	−1451.0	−4223.5	0.16	−4266.7	−273.1	186.7
		IGLO	−1451.0	−4223.5	0.16	−4266.7	−273.1	186.7
		LORG	−1451.0	−4223.5	0.16	−4266.7	−273.1	186.7
	TZ2P	CPHF	−1320.8	−3822.9	0.20	−3869.4	−295.7	202.7
		IGLO	−1320.8	−3822.9	0.20	−3869.4	−295.7	202.7
		LORG	−1320.8	−3822.9	0.20	−3869.4	−295.7	202.7
CF_2	DZP	CPHF	−109.7	−597.5	0.06	−508.0	77.6	101.4
		IGLO	−135.8	−590.5	0.00	−529.4	60.5	61.6
		LORG	−151.4	−573.7	0.01	−533.8	41.9	37.8
	TZ2P	CPHF	−131.8	−573.3	0.00	−514.0	60.3	58.4
		IGLO	−141.2	−568.9	0.03	−521.5	52.3	42.6
		LORG	−145.1	−564.6	0.03	−521.4	48.1	38.1
2	DZP	CPHF	−5.8	−409.5	0.71	−278.8	34.3	227.1
		IGLO	2.3	−444.3	0.50	−293.9	75.9	224.9
		LORG	−18.4	−435.9	0.58	−309.1	42.6	211.3
	TZ2P	CPHF	−43.0	−408.1	0.62	−315.0	9.3	176.8
		IGLO	−48.8	−415.1	0.54	−325.5	15.2	163.9
		LORG	−53.7	−410.5	0.58	−327.3	4.0	162.4
1	DZP	CPHF	22.1	−370.3	0.70	−224.7	59.3	231.9
		IGLO	7.3	−376.8	0.47	−243.9	73.3	192.6
		LORG	−17.5	−367.9	0.53	−262.8	39.5	170.8
	"*TZ2P*"[d]	CPHF	−4.2	−365.5	0.59	−247.9	45.8	189.4
		IGLO	−39.6	−350.5	0.51	−273.3	18.1	136.3
		LORG	−50.2	−341.5	0.53	−277.8	3.2	124.1
2·H^+	DZP	CPHF	88.9	178.3	0.35	50.1	8.7	207.8
		IGLO	100.7	157.4	0.26	34.4	62.1	205.7
		LORG	83.6	163.9	0.07	25.1	32.8	192.9
	TZ2P	CPHF	56.8	160.0	0.26	17.2	−10.3	163.5
		IGLO	52.3	150.1	0.11	7.9	−3.3	152.4
		LORG	47.1	154.1	0.20	6.1	−14.5	149.9
1·H^+	DZP	CPHF	114.2	168.4	0.50	86.0	30.2	226.5
		IGLO	59.7	129.1	0.65	44.6	−11.2	145.8
		LORG	46.7	126.2	0.66	32.4	−23.1	130.8
	"*TZ2P*"[d]	CPHF	91.6	145.4	0.44	64.4	21.9	188.6
		IGLO	49.8	121.6	0.69	37.0	−18.6	130.8
		LORG	43.4	115.9	0.75	33.7	−24.2	120.7
1	expt	CP/MAS	−23.2	−241	0.59	−184 (20)	9 (18)	104 (15)
1·H^+	expt	CP/MAS	49.4	68	0.84	45 (11)	7 (11)	94 (11)

[a] Shielding tensors are absolute in ppm. [b] Numbers in parentheses represent error in the last figures. [c] $\Delta\sigma$ and η are measures of the anisotropy: $\Delta\sigma = \sigma_{xx} - {}^1/_2(\sigma_{yy} + \sigma_{zz})$ and $\eta = 3(\sigma_{zz} - \sigma_{yy})/2\Delta\sigma$; σ_{xx} is chosen as σ_{ii} with the largest absolute deviation from the mean σ_{ii}'s, while σ_{yy} and σ_{zz} are chosen so that η is positive and ranges between 0 and 1. $\Delta\sigma$ is a measure of the overall anisotropy, and η approaches 0 if the anisotropy arises from a single tensor component. [d] The "*TZ2P*" basis set used for **1** and **1**·H^+ is TZ2P for C_2, $C_{4(5)}$, and $N_{1(3)}$, DZP for the methyl carbons, and DZ for H.

Table 3. LDFT-Calculated NMR Shielding Tensors and Anisotropies at Carbene Centers in $^1A_1$ CH_2, CF_2, **1**, **1**·H^+, **2**, and **2**·H^+ [a,b]

molecule	basis	method	σ_{iso}	$\Delta\sigma$[c]	η[c]	σ_{11}	σ_{22}	σ_{33}
CH_2	TZVP	IGLO	−1853.5	−5167.9	0.19	−5298.7	−461.4	199.7
		LORG	−1807.2	−5022.1	0.20	−5155.3	−461.4	195.2
CF_2	TZVP	IGLO	−114.1	−484.2	0.11	−436.9	29.0	65.7
		LORG	−130.5	−474.3	0.08	−446.7	15.6	39.5
2	TZVP	IGLO	−12.8	−300.8	0.83	−213.3	4.7	170.3
		LORG	−22.3	−318.1	0.74	−234.3	5.1	162.4
1	TZVP	IGLO	−2.4	−233.6	0.80	−158.2	13.3	137.6
		LORG	−10.4	−245.3	0.70	−174.0	14.0	128.9
2·H^+	TZVP	IGLO	66.9	126.7	0.23	34.2	15.1	151.4
		LORG	60.6	131.0	0.04	18.5	15.2	147.9
1·H^+	TZVP	IGLO	65.2	−84.4	0.88	68.8	8.9	117.9
		LORG	59.4	85.9	0.73	51.8	9.6	116.7
1	expt	CP/MAS	−23.2	−241	0.59	−184 (20)	9 (18)	104 (15)
1·H^+	expt	CP/MAS	49.4	68	0.84	45 (11)	7 (11)	94 (11)

[a] Shielding tensors are absolute in ppm. [b] Numbers in parentheses represent error in the last figures. [c] $\Delta\sigma$ and η are measures of the anisotropy. See footnote *c* in Table 2.

Local symmetry at the carbene center dictates the orientation of the principal components of the carbon shielding tensor. Although the experiments provide the magnitude and sign of the three principal components, they do not provide their alignment with respect to a set of molecular axes. In order to determine the alignment of the tensor components, *ab initio* electronic structure calculations were performed at the Hartree–Fock (HF) (Table 2) and local density functional (LDFT) levels (Table 3) on the parent imidazol-2-ylidene (**2**), **1**, :CF_2, and :CH_2. Although a singlet carbene wave function should be treated minimally by a 2 × 2 CI involving the in-plane lone pair and the out-of-plane p orbital at the carbene carbon,[7] previous calculations[49] on **2** have shown that the singlet wave function is reasonably well-represented by a single configuration. It should be noted that the singlet–triplet gap is very large for carbene **2**. Overestimation of calculated shielding tensor anisotropies has been reported for nitrogen shielding tensor calculations, where the nitrogen is involved in multiple bonding and has a lone pair.[50,51] Electron correlation has been suggested to be an important ingredient in the reliable calculation of such nitrogen chemical shielding tensors.

(49) Dixon, D. A.; Arduengo, A. J., III. *J. Phys. Chem.* **1991**, *95*, 4180.
(50) Schindler, M. *J. Am. Chem. Soc.* **1987**, *109*, 5950.
(51) Hinton, J. F.; Guthrie, P. L.; Pulay, P.; Wolinski, K.; Fogarasi, G. *J. Magn. Reson.* **1992**, *96*, 154.

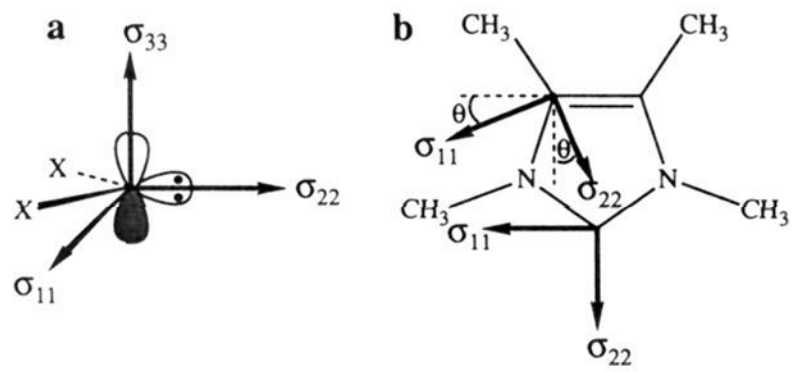

Figure 2. Shielding tensor primary component orientations in (a) **1**, **2**, $:CF_2$, and $:CH_2$ and (b) **1** and **1**·H^+ (σ_{33} is perpendicular to the molecular plane, and for the $C_{4(5)}$ centers θ has the following values: **1**, HF/"*TZ2P*"/LORG, θ = 10.5°; **1**, LDFT/TZVP/LORG, θ = 24.5°; **1**·H^+, HF/"*TZ2P*"/LORG, θ = 0°; **1**·H^+, LDFT/TZVP/LORG, θ = 3.6°).[52]

The calculated NMR shifts for all of the atoms in **1** are shown in Table 1. Those for the protons were obtained by averaging the three protons at each methyl. The agreement with experiment is better with the larger basis set and the LORG treatment of the gauge problem at the HF level. At the LDFT level, the LORG method seems to give values closer to experiment than does the IGLO method. Both the HF/"*TZ2P*"/LORG and DFT/TZVP/LORG calculations give reasonable predictions of the NMR shifts relative to TMS. The LDFT NMR shifts for the ring carbons are too low by ~17 ppm independent of whether the carbon is in the double bond or is the carbene center. Although the proton shifts are in the correct order, the values are too low and the splitting is too small at the HF level, whereas the opposite is true for the LDFT values.

One feature of the carbene shielding tensor that is evident without ambiguity from the calculations is its orientation, depicted in Figure 2, placing the most shielded component (σ_{33}) perpendicular to the plane of the molecule, the intermediate component (σ_{22}) along the direction of the carbene lone pair, and the least shielded component (σ_{11}) perpendicular to the other two within the plane of the molecule.

These tensor orientations are completely analogous to tensors determined for carbon nuclei with a hydrogen in place of the lone pair in aromatic environments[53] and for two-coordinate nitrogen[54–56] and phosphorus[57–59] nuclei possessing a lone pair. The calculated HF NMR tensor elements (Table 2) show an obvious basis set dependence as well as a dependence on the treatment of the gauge problem. The best gauge treatment is the LORG method, with the CPHF method providing the worst agreement (the CPHF method is affected most by the use of a finite basis). The use of the larger basis set also provides better agreement with experiment than does the use of the smaller DZP basis set. Although the HF results on **1** and **2** obviously show the directions of the tensor elements, the magnitudes are not correct for the least shielded component, although the magnitudes are predicted reasonably well for the other components. This is what one would expect, as the σ_{11} component corresponds to mixing the carbene lone pair into the nominally empty $2p_z$ orbital on the carbene, which should have the largest correlation correction. In order to better assess the role of correlation corrections, we also performed LDFT calculations, where some amount of correlation is treated in the wave function (Table 3). Following our expectations, the σ_{11} component is now in good agreement with the experimental values, as are the other components. We should point out that the calculated results are for an isolated gas-phase molecule at 0 K with no vibrational averaging nor medium effects, as compared to the experimental values, which were obtained in the solid at room temperature.

The calculated shifts and tensors for the parent imidazol-2-ylidene, **2**, show the need for including the methyl groups for comparison to experiment, even though the substituent variation is one atom removed from the carbene center. Although the trends in the tensor values are the same in **2** as in **1**, the values are not. The value of σ_{11} is smaller in **2** than in **1**, and the value of σ_{33} is larger in **2** than in **1**; only the value of σ_{22} is comparable between the two compounds.

More information about the carbene carbon NMR shift and the shielding tensors is available from examination of the theoretical results on the model systems $^1A_1$ $:CH_2$, $:CF_2$, and **2**. The results are given in Table 2 at the HF level and in Table 3 at the LDFT level. Although, the largest error is expected for $:CH_2$ at the HF level as this carbene has the largest coupling of the lone pair with the vacant p_z orbital, the results clearly show that an extremely low field shift is predicted for the carbene due largely to the very low value for σ_{11}. The value of the chemical shielding is a factor of at least 6 larger than the usual range given of ^{13}C shifts. The qualitative trend given by the HF shifts for $:CH_2$ is also found at the LDFT level. If fluorine is substituted for hydrogen in $:CH_2$, the ground state becomes a singlet and the singlet–triplet splitting becomes large. Difluorocarbene is now more like **1** (or **2**), and the value of σ_{11} becomes much larger (less negative) than in $^1A_1$ $:CH_2$. The value of σ_{22} also increases, while σ_{33} decreases. The extreme change in σ_{11} is a result of changes in the paramagnetic (deshielding) component of the tensor due to the much lower energy of the $n \rightarrow \pi^*$ transition in $^1A_1$ $:CH_2$ than $:CF_2$.[60] This change in the paramagnetic contribution to σ_{11} dominates the changes in the diamagnetic component (*vide infra*).

The chemical shielding tensor we have characterized for the carbene site in **1** represents one of the most anisotropic tensors reported for carbon in a strictly organic framework.[61] The negative value for σ_{11} in **1** suggests a continuing dominance of the carbene-like resonance structure A over the fully π-bonded ylidic resonance structure B. The value of σ_{11} in **1**, which is somewhat larger (less negative) than σ_{11} in $:CF_2$, is in accord with expectations of a dominant paramagnetic contribution to this tensor element.[62] A maximally π-bonded model is provided by the C_2 center in **1**·H^+, where the shielding tensor appears typical for π-bonded aromatic centers.[53] In fact the shielding tensor at C_2 of **1**·H^+ (Table 4) is

(52) Because the orientation of the chemical shielding tensor components is critical to the discussions of this work and the conventional assignments would allow σ_{11} and σ_{22} to vary with respect to the molecular axes, we have adopted, for the purposes of this article, a convention that allows the designations of the principal components of the chemical shielding tensors to remain approximately parallel to the assignments made at the carbene center in **1** and **2**. Thus as illustrated in Figure 2, σ_{22} at C_2 in the cations **1**·H^+ and **2**·H^+ remains along the C–H bond, with σ_{33} perpendicular to the molecular plane and σ_{11} orthogonal to the other two components (*i.e.*, parallel to the C_4–C_5 bond). At the $C_{4(5)}$ center in **1** and **1**·H^+, σ_{22} is the designation of the primary chemical shielding tensor component that is most nearly parallel to σ_{22} at C_2 and σ_{11} is the designation of the primary chemical shielding tensor component that is most nearly parallel to σ_{11} at C_2, while σ_{33} remains perpendicular to the molecular plane. The exact orientation of the primary chemical shielding tensor components at $C_{4(5)}$ is rotated by an angle θ (Figure 2) from the principal molecular axes.

(53) Mehring, M. *High Resolution NMR in Solids*; Springer-Verlag: Berlin, 1983.

(54) Wasylishen, R. E.; Power, W. P.; Penner, G. H.; Curtis, R. D. *Can. J. Chem.* **1989**, *67*, 1219.

(55) Wasylishen, R. E.; Penner, G. H.; Power, W. P.; Curtis, R. D. *J. Am. Chem. Soc.* **1989**, *111*, 6082.

(56) Curtis, R. D.; Penner, G. H.; Power, W. P.; Wasylishen, R. E. *J. Phys. Chem.* **1990**, *94*, 4000.

(57) Zilm, K. W.; Webb, G. G.; Cowley, A. H.; Pakulski, M.; Orendt, A. *J. Am. Chem. Soc.* **1988**, *110*, 2032.

(58) Duchamp, J. C.; Pakulski, M.; Cowley, A. H.; Zilm, K. W. *J. Am. Chem. Soc.* **1990**, *112*, 6803.

(59) Curtis, R. D.; Royan, B. W.; Wasylishen, R. E.; Lumsden, M. D.; Burford, N. *Inorg. Chem.* **1992**, *31*, 3386.

(60) The $^1A_1 \rightarrow {}^1B_1$ transition in $:CH_2$ is ~1.1 eV, see: Bauschlicher, C. W. *Chem. Phys. Lett.* **1980**, *74*, 273. Herzberg, G.; Johns, J. W. C. *Proc. R. Soc.* (London) Ser. A **1966**, *295*, 107. Shavitt, I. *Tetrahedron* **1985**, *41*, 1531. The $^1A_1 \rightarrow {}^1B_1$ transition in $:CF_2$ is ~4.3 eV; see: Comes, F. J.; Ramsay, I. A. *J. Mol. Spectrosc.* **1985**, *113*, 495. King, D. S.; Schenck, P. K.; Stephenson, J. C. *J. Mol. Spectrosc.* **1979**, *78*, 1.

(61) Duncan, T. M. *A Compilation of Chemical Shift Anisotropies*; Farragut Press: Chicago, 1990.

(62) A gas-phase UV spectrum of the perdeuterio-analog of **1** (taken at room temperature under autogenous pressure) shows a strong absorption at 236 nm and a weaker shoulder at ~270 nm. This latter absorption is possibly the $n \rightarrow \pi^*$ transition (4.6 eV).

Table 4. Summary Comparison of Experimental and Calculated Absolute Shielding Tensors for Ring Carbons in 1 and 1·H+ [a,b]

cmpd	atom	method	σ_{iso}	σ_{11}	σ_{22}	σ_{33}
1	C_2	expt SS CP/MAS	-23.2	-184 (20)	9 (18)	104 (15)
	$C_{4(5)}$	expt SS CP/MAS	61.7	67 (19)	-6 (22)	123 (17)
1·H+	C_2	expt SS CP/MAS	49.4	45 (11)	7 (11)	94 (11)
	$C_{4(5)}$	expt SS CP/MAS	56.7			
1	C_2	HF/"*TZ2P*"/LORG	-50.2	-277.8	3.2	124.1
	$C_{4(5)}$	HF/"*TZ2P*"/LORG	63.9	73.6	-19.2	137.2
1·H+	C_2	HF/"*TZ2P*"/LORG	43.4	33.7	-24.2	120.7
	$C_{4(5)}$	HF/"*TZ2P*"/LORG	53.2	55.0	-28.9	133.5
1	C_2	LDFT/TZVP/LORG	-10.4	-174.0	14.0	128.9
	$C_{4(5)}$	LDFT/TZVP/LORG	80.2	68.5	14.7	157.5
1·H+	C_2	LDFT/TZVP/LORG	59.4	51.8	9.6	116.7
	$C_{4(5)}$	LDFT/TZVP/LORG	59.1	39.0	-2.2	140.5

[a] Shielding tensors are absolute in ppm. [b] Numbers in parentheses represent error in the last figures.

Table 5. Paramagnetic (σ_{ii}^P) and Diamagnetic (σ_{ii}^D) Contributions to the Chemical Shielding Tensors at the Carbene Centers in Various Carbenes [a,b]

cmpd	σ_{iso}	$\sigma_{11}^P/\sigma_{11}^D$	$\sigma_{22}^P/\sigma_{22}^D$	$\sigma_{33}^P/\sigma_{33}^D$
CH_2	-1807.2	-5431.6/276.4	-732.3/270.9	-99.3/294.5
CF_2	-130.5	-711.1/264.3	-333.2/348.9	-300.5/340.0
1	-10.4	-441.0/267.0	-405.9/419.9	-262.0/390.9
1·H+	59.4	-264.5/316.3	-413.7/423.5	-323.1/439.8

[a] Shielding tensors are absolute in ppm for the LDFT/TZVP/LORG calculations. [b] Data for 1·H+ are for C_2.

very similar to the tensors at the $C_{4(5)}$ centers of both 1·H+ and 1.[52] Experimental and theoretical electron distribution determinations[9] on 1 show these $C_{4(5)}$ centers to be strongly π-bonded compared to C_2 in 1 agreeing with expectations based on these shielding tensors.

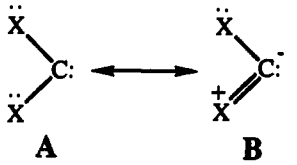

A B

The experimental and "best" calculated absolute shielding tensors and components for the ring carbons in 1 and 1·H+ are summarized in Table 4. The uniqueness of the chemical shielding tensor at the carbene center of 1 is obvious. The LDFT/TZVP/LORG calculations appear to have the best overall match with experimentally determined values. The similarity of the C_2 center in 1·H+ with the $C_{4(5)}$ centers in both 1·H+and 1 indicates that a more typical π-bonded arrangement is found at this center compared to the situation in 1.

The three components to the shielding tensor, σ_{11}, σ_{22}, and σ_{33}, at the carbene center in 1 are comprised of both a paramagnetic contribution (deshielding) and a diamagnetic contribution (shielding). These contributions are broken out in Table 5 for the DFT/TZVP/LORG calculations. As noted above the σ_{11} tensor component is very small (large negative) as the result of dominant paramagnetic contributions arising from the low-energy $n \rightarrow \pi^*$ transition at the carbene center. The paramagnetic contribution to σ_{11} decreases (σ_{11}^P becomes less negative) as the $n \rightarrow \pi^*$ energy gap increases.[60,62] The diamagnetic contribution to σ_{11} is remarkably similar for $^1A_1$:CH_2, :CF_2, and 1. Like the situation with σ_{11}, the paramagnetic contribution to σ_{22} also decreases on going from $^1A_1$:CH_2 to :CF_2 but then increases slightly for 1. The diamagnetic contribution to σ_{22} steadily increases through the carbene sequence. The changes to the paramagnetic contribution to σ_{33} show an increase on going from $^1A_1$:CH_2 to :CF_2 but again decrease somewhat for 1. The changes in σ_{33}^D follow the trends for σ_{22}^D. The increases in the total diamagnetic shielding through the sequence $^1A_1$:$CH_2 \rightarrow$: $CF_2 \rightarrow$ 1 are in accord with a recent experimental electron density determination on the perdeuterio-analog of 1 and further reflect the reactivity trend from predominantly electrophilic for $^1A_1$:CH_2 to predominantly nucleophilic for 1.[9] The total diamagnetic shielding is greatest for 1·H+, which also correlates with expectations of increased π-bonding at C_2 relative to the situation in 1.[9]

An NMR measurement which has been useful in characterizing delocalization in the imidazole ring system is the chemical shift of protons directly attached at $C_{4(5)}$.[13,63-69] The methyl substitution in 1 and 1·H+ precludes such observations for these molecules, but the model compounds 2 and 2·H+ do bear protons at $C_{4(5)}$. It is worthy of note that the predictions of chemical shifts for $H_{4(5)}$ in the model compounds 2 and 2·H+ are in accord with observations reported previously for 1,3-di(1-adamantyl)imidazol-2-ylidene (δ $H_{4(5)}$ = 6.9) and 1,3-di(1-adamantyl)imidazolium chloride (δ $H_{4(5)}$ = 7.9).[13] This $\Delta\delta$ of 1 ppm, which places the imidazole ring protons in 1,3-di(1-adamantyl)imidazol-2-ylidene upfield of their resonance in the imidazolium ion, suggests that the carbene does not experience as high a degree of delocalization as the carbenium ion. The calculation of the ^1H chemical shielding is particularly hampered by neglect of solvent effects and the assumption of a stationary 0 K geometry. Nonetheless, from the HF/TZ2P/LORG calculations we predict δ $H_{4(5)}$ = 6.2 for 2 and δ $H_{4(5)}$ = 6.9 for 2·H+. These values give a $\Delta\delta$ of 0.7 ppm for $H_{4(5)}$ in 2 and 2·H+, which is remarkably close to the analogous experimental value for the adamantyl-substituted system.

Conclusion

The carbene site in 1 possesses a large chemical shielding anisotropy, and we anticipate this to be the case for most singlet carbenes. The theoretical results clearly show that electron correlation must be treated in *ab initio* calculations of the electronic character of singlet carbenes. As demonstrated by the differences in the predictions for 1 and 2 in which methyl substituents are replaced by hydrogens, for theoretical models of the chemical shielding tensor to correctly predict the experimental values it is necessary to include substituents that are present on the experimentally studied molecules. This can even be an important consideration when the substituents are not directly attached to the center whose chemical shielding tensor is being calculated, as with the carbene centers in 1 and 2. The orientation of the carbene chemical shielding tensor in 1 is predicted to be identical to tensors characterized for other nuclei in similar electronic environments, such as nitrogen and phosphorus, which

(63) Arduengo, A. J., III; Burgess, E. M. *J. Am. Chem. Soc.* **1976**, *98*, 5021.
(64) Janulis, E. P., Jr.; Arduengo, A. J., III. *J. Am. Chem. Soc.* **1983**, *105*, 3563.
(65) Arduengo, A. J., III; Kline, M.; Calabrese, J. C.; Davidson, F. *J. Am. Chem. Soc.* **1991**, *113*, 9704.
(66) Arduengo, A. J., III; Dias, H. V. R.; Calabrese, J. C.; Davidson, F. *J. Am. Chem. Soc.* **1992**, *114*, 9724.
(67) Arduengo, A. J., III; Dias, H. V. R.; Calabrese, J. C.; Davidson, F. *Inorg. Chem.*, **1993**, *32*, 1541.
(68) Arduengo, A. J., III; Dias, H. V. R.; Davidson, F.; Harlow, R. L. *J. Organomet. Chem.* **1993**, *462*, 13.
(69) Arduengo, A. J., III; Dias, H. V. R.; Calabrese, J. C.; Davidson, F. *Organometallics* **1993**, *12*, 3405.

routinely occur at two-coordinate sites possessing lone pairs. The most shielded component of the tensor, σ_{33}, is perpendicular to the molecular plane. There is an intermediate tensor component, σ_{22}, along the direction of the carbene lone pair of electrons. There is a strongly deshielded tensor component, σ_{11}, that is normal to the other two components. The σ_{11} tensor component has a large paramagnetic contribution from the low-lying n $\rightarrow \pi^*$ transition at the carbene center.

The comparison of the chemical shielding anisotropy in **1** and **1**·H^+ indicates that the carbene-type anisotropy in **1** is absent in **1**·H^+, where an anisotropy typical of π-bonded sp^2 carbon centers is observed.

The chemical shielding anisotropy in **1** which appears typical for singlet carbenes is consistent with an electron density distribution determined for the perdeuterio-analog.

Acknowledgment. W.P.P. acknowledges NSERC of Canada for a postdoctoral fellowship. This research was supported in part by NSF (K.W.Z.) under Operating Grant CHE-9018455 and Instrument Grant CHE-9115967, which allowed the acquisition of the computing facilities at Yale used for the experimental work. We also appreciate helpful conversations with Professor J. D. Roberts and Fredric Davidson.